IL NUOVO CIMENTO **44 C** (2021) 21
DOI 10.1393/ncc/i2021-21021-x

COMMUNICATIONS: SIF Congress 2020

Random telegraph noise investigation in irradiated digital SiPMs

M. CAMPAJOLA(1)(2)

(1) *Dipartimento di Fisica, Università degli Studi di Napoli "Federico II" - Napoli, Italy*
(2) *INFN, Sezione di Napoli - Napoli, Italy*

received 1 February 2021

Summary. — Digital SiPM is a very attractive solution for single-photon detection due to its excellent timing resolution and the additional pixel circuitry capability for signal processing. Possible applications often require the device to be operated in a high-radiation environment. In this work, we investigate the degradation of the device performances after irradiation with protons. We report on the increase of the dark count rate level and the random telegraph noise occurrence, *i.e.*, the discrete switching of the dark count rate between two or more values. Results have been compared with the most accurate models proposed in the literature.

1. – Introduction

Photon-counting applications usually require very stringent performances, such as high Photon Detection Efficiency (PDE), good timing resolution and low Dark Count Rate (DCR). Vacuum Photo-multiplier Tubes (PMTs) performed this task excellently for years, however, with some disadvantages in terms of system reliability, complexity and high cost. Furthermore, they are not suitable for mass production. In recent times, Single-Photon Avalanche Diodes (SPADs) proved to be a valid alternative compared to PMTs in various photon counting applications, such as High-Energy Physics (HEP) experiments, medical imaging, and Light Detection and Ranging (LIDAR). A SPAD consists of a PN junction biased above the breakdown voltage, thus operating in Geiger mode. It is capable of a substantial internal gain ($G \sim 10^6$) with no need for pre-amplification, resulting in a single-photon sensitivity. Furthermore, SPADs provide excellent timing and spatial resolutions, reaching a few tens of picoseconds and micrometers, respectively. A widely used type of solid state photo-detector is the Silicon Photo-Multiplier (SiPM), which consists of an array of SPADs connected in a parallel configuration. SiPM demonstrated excellent characteristics, such as high PDE, excellent timing, moderate DCR, and linearity in response to the number of incident photons over a wide range [1]. Recently, SPAD-based pixel arrays fabrication has been demonstrated even in CMOS technology. The CMOS fabrication processes paved the way to the realization of arrays of SPADs integrated with the signal processing circuitry on the same silicon substrate. Such a monolithic device is often reffed to as a "digital SiPM". In contrast to conventional SiPMs, the digital SiPMs provide the SPAD signals digitization on chip and thanks to the implementation of integrated circuitry, like control logic, trigger network, time-to-digital converter (TDC), produce faster and more accurate photon counts with extremely well-defined timing [2]. Moreover, each SPAD is read out individually, thus allowing for spacial resolution down to the SPAD sizes. Although digital SiPMs offer many advantages, they have the drawback of a reduced fill-factor due to the integrated electronics and a worse DCR due to more complex processing and not yet fully optimized CMOS fabrication steps for SPAD design.

Many applications would benefit from the usage of digital SiPMs, like HEP experiments, Positron Emission Tomography (PET) and LIDAR. Digital SiPMs are very promising detectors even for space missions, considering their low power dissipation and the possibility of compactness. Such applications often require the detector to operate in a harsh radiation environment. For photo-sensor devices, a key issue is the dark current or the DCR increase with the radiation dose [3]. Studies related to radiation-induced effects also showed in many cases the appearance of discrete fluctuations of the dark current between two or more levels after irradiation. Such effect is referred to as Random Telegraph Noise (RTN) and could be a serious issue for the correct operation of the devices. RTN is related to radiation-induced defects in the device silicon bulk or at the SiO_2/Si interfaces. Several studies have been carried out to understand in detail this phenomenon over a large variety of devices, but its origin is still controversial to date.

The goal of this work is to present an in-depth analysis of the RTN behaviours observed in a digital SiPM device irradiated with protons. The key parameters of the RTN, such as the number of discrete DCR levels, the switching frequency, the amplitude between levels, its activation energy and its annealing temperature have been characterized in order to obtain some useful information on the defects involved in such a phenomenon.

2. – Noise sources

A critical issue in SPAD performances is related to the high DCR level. Dark counts are induced by *e*-*h* carriers generated in the device sensitive volume even in total darkness conditions, which result in carrier avalanches completely indistinguishable from the photo-generated ones. One of the main processes responsible for such a phenomenon in SPADs is the thermal generation of free carriers: thermally excited electrons passing from valence to conduction band. Direct transitions are rare at room temperature because of the large and indirect silicon band-gap. However, mid-gap levels introduced by crystal defects or impurities can act as intermediate states and facilitate the transition to the conduction band. This process is fully described by the Shockley-Read-Hall (SRH) model [4], which provides the following expression for the generation rate G_{SRH}:

$$G_{SRH} = \frac{n_i}{2\cos h(\frac{E_0-E_t}{k_B T})} N_t \sigma v_{th}, \tag{1}$$

where n_i is the intrinsic carrier concentration in silicon, E_0 is the Fermi level, E_t is the energy level of the trap, N_t is the trapping center concentration, σ is the capture cross section of the trap for electrons or holes and v_{th} is the thermal velocity of the carriers. From this equation, it is clear that the generation rate is maximum when the trap energy E_t is equal to the Fermi level E_0, indicating that only traps whose energy levels are near the mid-gap act as effective e-h generation-recombination (G-R) centers. By integrating the thermal generation rate G_{SRH} times the probability for an e-h to trigger an avalanche (BD_P) over the depletion region, one obtains the thermal contribution to the total DCR. In the presence of a strong electric field, such as for the SPAD case, even tunnelling effects can contribute to the total generation rate. Specifically, band-to-band or trap-assisted tunneling mechanisms may occur, enhancing the total DCR [5].

Defects and impurities responsible for the DCR enhancing can be induced in the device not only in the manufacturing process but also during its operation. This is the case of detectors employed in a radiation-full environment. A relevant part of radiation-induced effects in silicon devices is due to the so-called "displacement damage": it consists of the displacement of silicon atoms from their lattice position caused by the interaction with high-energy particles. As a consequence of such a process, a Vacancy (V) is formed, being the absence of an atom from its normal lattice position. Such a one-atom disorder in a crystalline lattice is called "point defect". Depending on the mass and the energy of the incident particles, the primary displaced atoms can have enough energy to cause further displacements. In such a case, a dense agglomerate of defects, denoted as "defect cluster", is formed. Vacancies created during irradiation may migrate inside the material and interact with each other or with impurity or dopant atoms and form more complex and stable defects, thus resulting in the increase of the dark count rate.

In very small electronic devices, where only a few carriers are involved in the operations, individual defect sites or clusters of defects, that are responsible for DCR, may also give rise to a discrete switching between two or more DCR levels. Such a phenomenon is called Random Telegraph Noise (RTN). In the last two decades, RTN has been investigated in small-scale MOSFET [6], and image sensors like charged coupled devices [7] and active pixel sensors [8, 9]. In small geometry MOSFET, RTN is due to the trapping and emission of channel carriers by oxide traps. When a charge carrier is trapped, the MOSFET channel conductance is instantaneously reduced. When this electron is emitted, the channel conductance goes back to its original value leading to a discrete fluctuation of the transconductance. Many works attributed the origin of the $1/f$ noise observed in larger area devices to such discrete conductance fluctuations [10]. In photo-sensors like SPADs, RTN is usually attributed to random changes of the G-R rate caused by charge or structural changes of complex defects located inside the depleted volume. The high and low DCR states would correspond to some defect re-configuration inducing a high and low e-h generation rate, respectively.

Irrespective of the defect originating such effect, the conceptual scheme of the physical mechanism producing the DCR modulation can be depicted as shown in fig. 1. Here we assumed that the G-R centre can exist in two states, separated by an energy barrier. The switching from a stable state to another, due to thermal fluctuations, would produce the RTN behaviours.

3. – Experimental setup

The device under test has been designed and implemented in a 150 nm CMOS process and provided by Fondazione Bruno Kessler (Trento, Italy). It includes several architectures of SPADs with different sizes (10, 15, 20 μm) and two junction layouts. One layout is based on an asymmetric abrupt P+/Nwell junction enclosed in a low-doped region, in order to create a guard-ring and avoid premature edge breakdown; a second layout includes a graded Pwell/Niso junction. Each SPAD is integrated together with its relative front-end pixel circuit. The voltage pulse from the SPAD is discriminated by

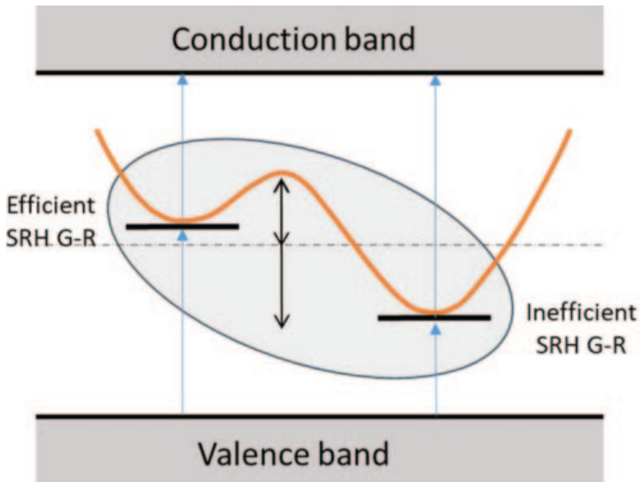

Fig. 1. – Conceptual scheme of the mechanism originating the random telegraph noise.

Schmitt-trigger comparator resulting in digital signal output. A control logic allows to connect one SPAD at the time to the output (see fig. 2). More details about the device design are given in [11].

The samples have been irradiated with protons by using a 14 MV Tandem accelerator and a Superconducting Cyclotron (SC) able to accelerate protons up to 62 MeV, at the *Laboratori Nazionali del Sud (LNS) - Istituto Nazionale di Fisica Nucleare (INFN)* in Catania (Italy). We irradiated one sample with 60 MeV protons up to a Displacement Damage Dose (DDD) of 115 TeV/g and another sample with 21 MeV protons up to a DDD of 376 TeV/g. The irradiation has been performed at room temperature and the samples were kept unbiased during the irradiation. In table I we report the DDD and the Total Ionizing Dose (TID) levels accumulated during the irradiation.

4. – RTN occurrence

In order to investigate the presence of RTN before and after irradiation, several hours of continuous DCR measurements have been performed for each of the investigated

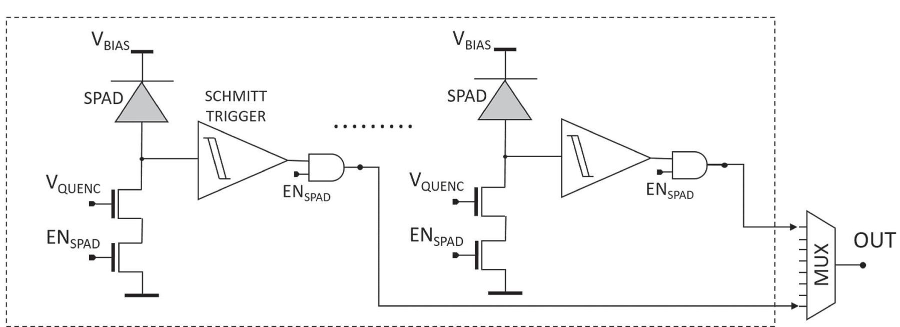

Fig. 2. – SPAD readout electronics within the device under test.

TABLE I. – *Irradiation test summary: delivered fluences and doses.*

Sample ID	Proton fluence $[p/\mathrm{cm}^2]$	Energy [MeV]	TID [krad]	DDD [TeV/g]
1	2.90×10^{10}	60	5.0	115
2	5.63×10^{10}	21	17.5	376

SPADs. Before irradiation, mean DCR values stay around $\mathcal{O}(1\,\mathrm{kcps})$ for a $10 \times 10\,\mu\mathrm{m}^2$ active area SPAD, with only a small fraction of SPADs showing some DCR discrete fluctuations (less than 5%).

After irradiation, a significant DCR increase, almost proportional to the delivered displacement damage dose, was observed. This has been deeply investigated in refs. [12-15]. Furthermore, a very large fraction of the irradiated SPADs showed the occurrence of RTN effects. They appear as discrete DCR fluctuations between two or more levels. As an example, in fig. 3 we report a 5 minute acquisition frame of the DCR for 6 SPADs: (a) shows a standard DCR behaviour; (b), (c) and (d) show bi-stable behaviours; (e) and (f) show multi-stable behaviours. In table II and table III, we summarize the number SPADs affected by RTN effects in the two different SPAD layouts. The results indicate that RTN occurrence depends on the accumulated DDD. Furthermore, a higher RTN occurrence probability has been observed in the P+/Nwell layout with respect to Pwell/Niso.

The RTN occurrence increases with the SPAD active area as shown in fig. 4 (left). This is not surprising, because of the higher probability for protons to interact and produce displacement damage with a larger-area SPAD. Moreover, we observed a correlation with the SPAD DCR values: the most damaged SPADs (those with the higher DCR) present RTN effects with higher probability, as shown in fig. 4 (right).

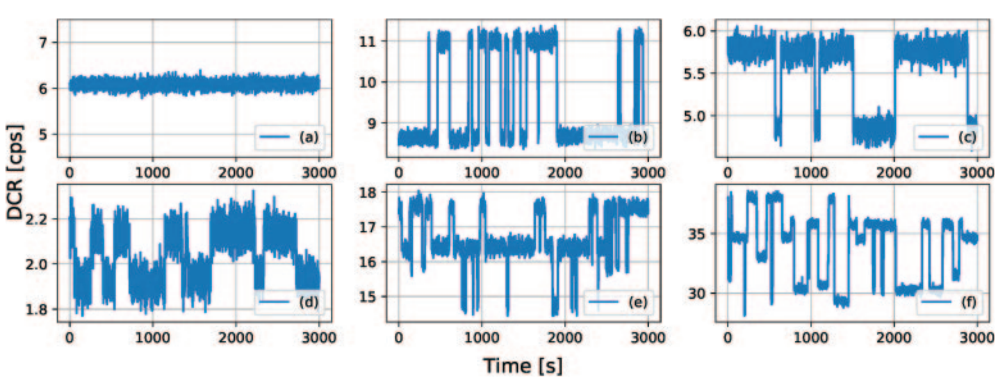

Fig. 3. – Example of typical DCR time-frame acquisitions on irradiated SPADs: (a) shows the standard DCR behaviour of a SPAD not affected by RTN; (b), (c), (d) show a two-level RTN behaviour, while (e) and (f) a multi-level RTN.

TABLE II. – *RTN occurrence in a device irradiated with a DDD = 115 TeV/g.*

Layout	Analysed SPADs	RTN SPADs	2 levels	3 levels	Multi levels (≥ 4)	RTN SPADs fraction
P+/Nwell	120	72	22	11	41	60%
Pwell/Niso	338	139	41	10	88	41%

TABLE III. – *RTN occurrence in a device irradiated with a DDD = 376 TeV/g.*

Layout	Analysed SPADs	RTN SPADs	2 levels	3 levels	Multi levels (≥ 4)	RTN SPADs fraction
P+/Nwell	154	116	17	11	97	75%
Pwell/Niso	339	203	40	10	153	60%

5. – RTN characterization

On a sub-set of SPADs affected by two-level DCR fluctuations, we deeply investigated the RTN behaviours. A two-level RTN can be simply characterized by 3 parameters, namely, the time spent in the high-DCR level (T_{up}), the time spent in the low-DCR level (T_{down}), and the RTN amplitude, *i.e.*, the difference between the two DCR levels (fig. 5). We analyzed the distributions of time in which the SPAD remains in the high- and low-DCR state (fig. 6). The exponential behaviour is in accordance with the hypotheses of a Poisson stochastic process regulating the DCR switching events [16, 17]. For such a particular SPAD, the time constants obtained from the fit are: $\tau_{up} = 115$ s and $\tau_{down} = 117$ s.

5·1. *Temperature dependence.* – From measuring the RTN behaviours at different temperatures, useful information about the physical process originating its mechanisms can be gained. For this purpose, we performed long-time DCR measurements on two-level RTN SPADs at temperatures in the range [15 °C–45 °C] by means of a climatic chamber.

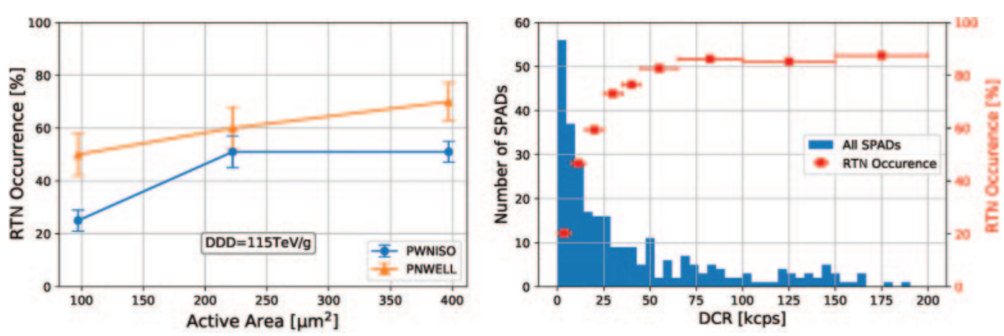

Fig. 4. – Left: RTN occurrence as a function of the SPAD active area for SPADs irradiated with 115 TeV/g. Right: DCR distribution and related RTN occurrence.

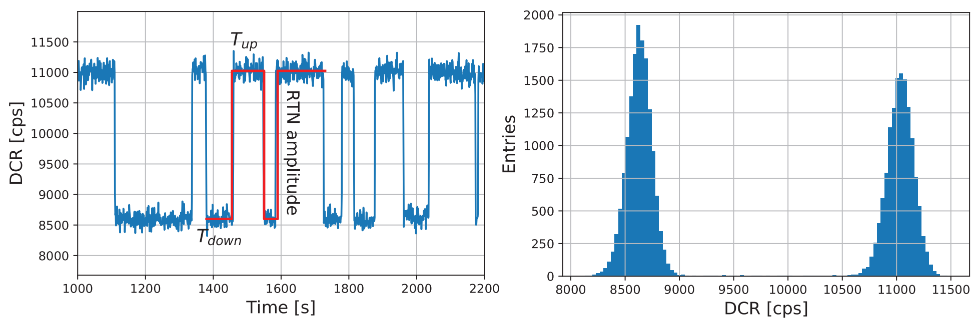

Fig. 5. – DCR in a SPAD affected by a two-level RTN. Left: time frame of the DCR acquisitions. Right: histograms of the DCR values; here, two separated DCR population corresponding to the two RTN levels can clearly be observed.

In fig. 7, we report the DCR time-frame acquisition of a typical two-level RTN SPAD at different temperatures. It can be clearly observed that, as the temperature decreases, the mean DCR level as well as the RTN amplitude and the switching probability decrease too. It is to point up that an accurate measurement of the time constants as a function of the temperature required a collection of hundreds of RTN transitions, meaning many days of acquisition at the lower temperatures.

In fig. 8, we report the time constants and the RTN amplitude as a function of the temperature, measured on a two-level RTN in a P+/Nwell and a Pwell/Niso SPADs. The temperature dependence of the measured time constants (τ_{up}, τ_{down}) is well described by the Arrhenius law:

$$\frac{1}{\tau} = C\, e^{(-E_a^{RTN}/k_\mathrm{B}T)}, \tag{2}$$

where C is a constant, and E_a^{RTN} is the RTN switching activation energy.

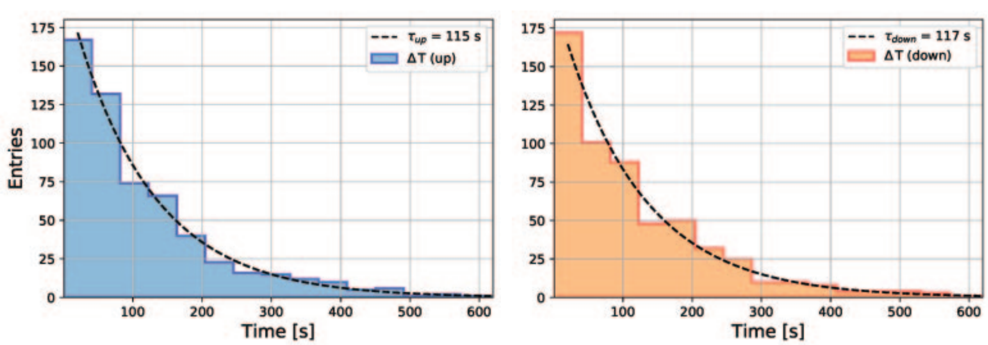

Fig. 6. – Histograms of the time intervals spent in the high- and low-DCR states in a SPAD affected by two-level RTN fluctuations. The dashed lines represent the best fits curves obtained by fitting data with the function $1/\tau \cdot \exp(-t/\tau)$.

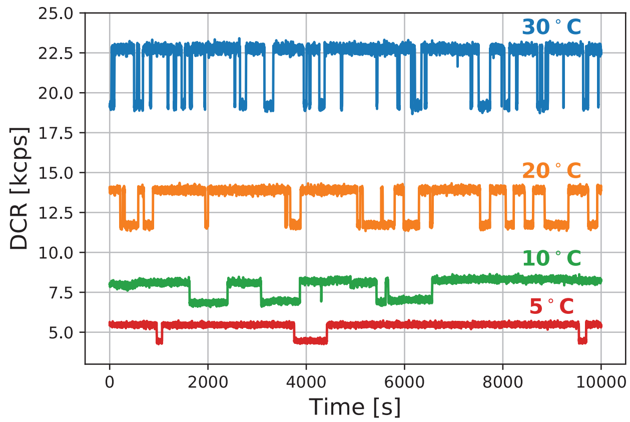

Fig. 7. – Two-level RTN fluctuation for a given SPAD at different temperatures.

For both structures, mean activation energy values near 0.8–0.9 eV have been measured. Such a strong activation energy suggests the presence of defects with two stable states separated by an energy barrier. The switching from a meta-stable state to another would occur with thermal fluctuations.

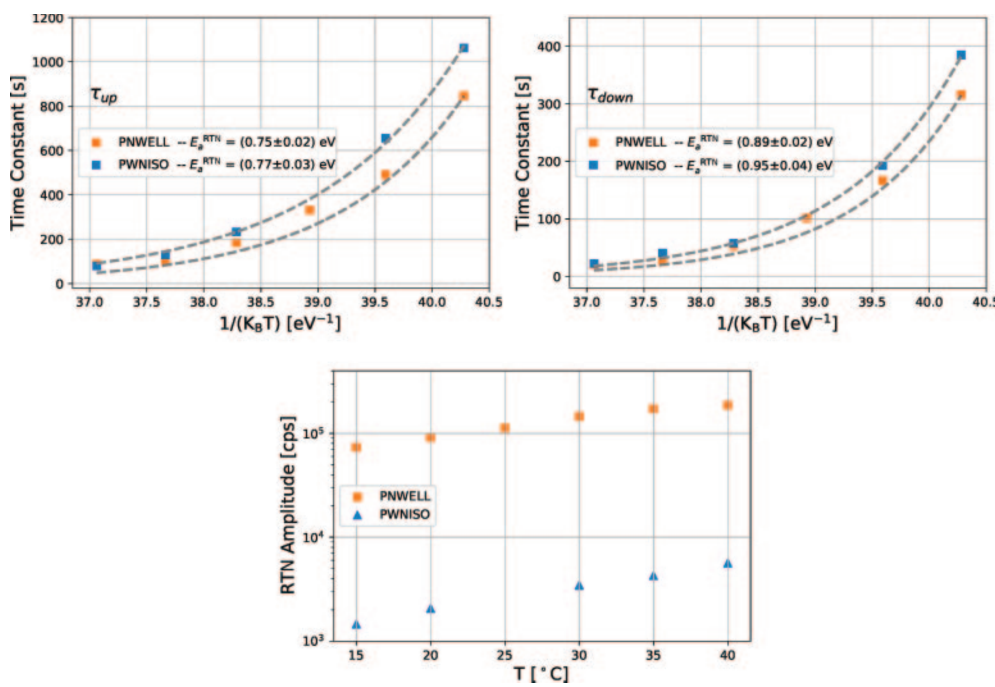

Fig. 8. – RTN behaviours in two SPADs with different layouts. On the top: time constants as a function of $1/K_{\mathrm{B}}T$ for *up* and *down* levels. On the bottom: RTN amplitude as a function of the temperature.

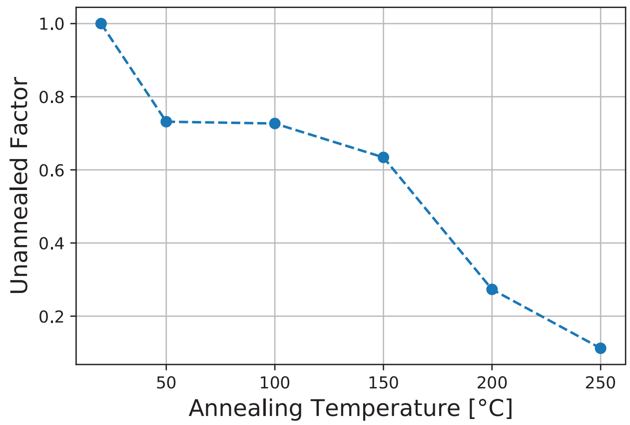

Fig. 9. – Fraction of unannealed RTN SPADs as a function of the annealing steps.

6. – Annealing

By performing a high-temperature isochronal annealing, important information about RTN origin can be obtained. Indeed, the annealing procedure is a useful tool for a deep study of the radiation-induced defects. Following ref. [18], the detection of preferential annealing temperature allows to identify the defects involved in the DCR-generation mechanisms. We keep our samples for one hour at temperatures in the range [50 °C–250 °C] with a 50 degree step. After each step, especially at temperatures highers than 150 °C, we observed a strong reduction of the number of SPADs affected by RTN, meaning that the defects responsible for the RTN fluctuations have been annealed [19]. In fig. 9, we report the unannealed factor, *i.e.*, the ratio between the number of remaining SPADs with RTN and the total number of SPADs with RTN measured before the annealing procedure, as a function of the annealing steps.

7. – Discussion

In the literature different explanations of the RTN effect in photo-diodes exist (see ref. [8] for a comprehensive review). Among these, di-vacancies (V-V) are often invoked to explain RTN through a mechanism called "intercenter charge transfer": the proximity of di-vacancies within defect clusters may result in a charge transfer; as a consequence of the change in the charge state, the generation rate can be enhanced. Di-vacancy defects can move in different positions with respect to each other and the probability to have the intercenter transfer can change from one configuration to another, causing the switching of the DCR. On the other hand, in a phosphorus-doped device, like the devices under test, the vacancies created by proton-induced silicon displacement could produce P-V center defects. The P-V defect has a dipole structure and can reorient its axis when the vacancy moves in one of four Si atoms close to the P atom. This new position corresponds to a new defect energy level, which could be at the origin of the RTN behaviour.

The greater RTN occurrence observed in the P+/Nwell junction with respect to the Pwell/Niso structure, as reported in tables II and III, would support the P-V center hypothesis. Indeed, the higher doping profile of the former structure would result in an overall increase of the P-V complex defect concentration. In ref. [20], the activation energy related to the P-V reorientation mechanism was estimated to be $\sim$0.93 eV. The values measured in the current work for the time constant activation energy for both SPAD layouts are in the range [0.75–0.95] eV and therefore compatible with the hypothesis of a P-V defect originating the observed RTN. Furthermore, from the annealing procedure, it was observed how most of the RTN SPADs anneals at a temperature between 100 °C and 200 °C (see fig. 9). This strongly supports the hypothesis of P-V centers being responsible for RTN, as their annealing temperature is about 140 °C, while V-V defects require a temperature exceeding 300 °C [18].

8. – Conclusions

Many recent experimental results reported the observation of discrete fluctuation of the dark current over a large variety of irradiated CMOS image sensors. Such results suggest that metastable G-R centers are the norm in irradiated photo-detectors. This work aims to provide a characterization of the DCR behaviours in a proton-irradiated digital SiPM. Digital SiPMs offer the possibility to access the single SPAD output and, therefore, to observe in detail the characteristics of the DCR. Furthermore, since the amplification in SPADs is internal, they offer the best sensitivity to study the properties of G-R centers. After irradiation, besides an overall increase of the DCR, the appearance of an RTN behaviour in most of the SPADs has been observed. We performed a set of different measurements to characterize the defects responsible for RTN. The measurements reported in this work seem to support the hypothesis that attributes the RTN feature to the reorientation of phosphorus-vacancy centers. However, further investigations are certainly necessary to gain a better understanding of this phenomenon.

REFERENCES

[1] Piemonte C. and Gola A., *Nucl. Instrum. Methods A*, **926** (2019) 15.
[2] Palubiak D. P. and Deen M. J., *IEEE J. Sel. Top. Quantum Electron.*, **20** (2014) 426.
[3] Srour J. R. and Palko J. W., *IEEE Trans. Nucl. Sci.*, **60** (2013) 1740.
[4] Shockley W. and Read W. T., *Phys. Rev.*, **87** (1952) 835.
[5] Xu Y. *et al.*, *Solid-State Electron.*, **129** (2017) 168.
[6] Zhongming Shi J. *et al.*, *IEEE Trans. Nucl. Sci.*, **41** (1994) 1161.
[7] Hopkins I. H. *et al.*, *IEEE Trans. Nucl. Sci.*, **40** (1993) 1567.
[8] Bogaerts J. *et al.*, *IEEE Trans. Nucl. Sci.*, **49** (2002) 249.
[9] Virmontois C. *et al.*, *Solid-State Electron.*, **49** (2002) 249.
[10] Andersson G. I. *et al.*, *J. Appl. Phys.*, **72** (1992) 2680.
[11] Pancheri L. *et al.*, *Proc. ESSDERC*, **2011** (2011) 179.
[12] Campajola M. *et al.*, *Nucl. Instrum. Methods A*, **947** (2019) 162722.
[13] Campajola M. *et al.*, *JINST*, **15** (2020) C08017.
[14] Campajola M. *et al.*, *Proc. SPIE Int. Soc. Opt. Eng.*, **11454** (2020) 1145409.
[15] Campajola M. *et al.*, *J. Phys.: Conf. Ser.*, **1226** (2019) 012007.
[16] Kirton M. J. *et al.*, *Adv. Phys.*, **38** (1989) 367.
[17] Di Capua F. *et al.*, *IEEE Trans. Nucl. Sci.*, **65** (2018) 1654.
[18] Watkins G. D. *et al.*, *Mater. Sci. Semicond. Process.*, **3** (2000) 227.
[19] Di Capua F. *et al.*, *Sci. Rep.*, **11** (2021) 8580.
[20] Watkins G. D. *et al.*, *Phys. Rev.*, **134** (1964) A1359.